Bulletin of the Earthquake
Research Institute
Vol. 42 (1964), pp. 631-647

35. *Studies of the Thermal State of the Earth. The 15th Paper: Variation of Thermal Conductivity of Rocks. Part 1.*

By Kaoru Kawada,

Earthquake Research Institute.

(Read Mar. 27, 1964.—Received Sept. 30, 1964.)

Abstract

Thermal conductivity of dunite, peridotite, eclogite, hornblende-gabbro, basalt, serpentinized-peridotite, quartz-diorite, diorite and slate are measured in a temperature range 100°*C*~600°*C* by a modified divided bar method. The reference substance used is nickel of which thermal conductivity was calibrated against crystalline quartz and fused silica. Thermal conductivity of all the rocks studied decrease with temperature increase. The results are interpreted in terms of the phonon conduction theory and are used for determining the upper and lower limits of temperature at the Moho discontinuity beneath Japan.

1. Introduction

Knowledge of the thermal and pressure variations in the conductivity of rocks is important for the thermal problems of the earth: problems such as the thermal history of the earth, the terrestrial heat-flow, and the temperature distribution in the earth's interior depend critically upon the thermal conductivity of rocks at elevated temperatures and pressures.

An investigation of the thermal conductivity of rocks at temperatures between 0 and 500°*C* was carried out by Birch and Clark[1], and it was found that normally the conductivity decreases with the temperature increase. According to Bridgeman's experiments, the thermal conductivity of rocks increases with the pressure increase at a rate of a few percent per 10 *kilobars*[2].

It is now a matter of great importance to make a study of the

1) F. Birch, and H. Clark, *Amer. J. Sci.*, **238** (1940), 529 and 613.

2) P. W. Bridgeman, *The Physics of High Pressure*, (G. Bell and Sons, London, 1949), Ch. 11.

thermal conductivity at temperatures higher than those covered by the investigation of Birch and Clark. The reason for this is that the actual temperature in the earth's deep interior is believed to be much higher and, moreover, suggestions have been made that the radiative and excitonic conduction of heat may exceed the phonon conduction at temperatures higher than 1200°*C* or so[3)4)]. It is the intention of the present writer to study the thermal conductivity of rocks at those temperatures that pertain to the main part of the earth's mantle and to establish whether or not the radiative *and/or* excition transfer of heat is really effective in the earth's mantle. Radiative and excitonic heat transfer in the earth has been discussed only from theoretical grounds so far.

To start with, however, it was considered to be proper to extend the temperature range from below. In the present study, it was intended to measure the variation of the thermal conductivity of those rocks, which are considered to be the representative components of the earth's crust and upper mantle in the temperature range 100°*C* to 600°*C*. This temperature range largely overlaps with that covered by Birch and Clark 24 years ago. It is hoped, however, that this preliminary work will constitute the first stage of the scheduled further investigation into higher temperature ranges.

2. Apparatus and Method

2-1. Apparatus

The method of measurement employed in the present study is a comparative method called the divided bar method, which has been used by many geophysicists for measuring the thermal conductivity of rocks at room temperature. The original type of the divided bar apparatus was developed by Benfield[5)], and Fig. 1 is a schematic diagram of the original apparatus. As shown in the figure, the specimen (R) cut in the form of a disk is inserted between two metal (brass) bars (R_a) and (R_b). At the top of the upper metal bar, an electric heater produces a constant heat which flows down through the bars and specimen. The lower end of the lower bar is cooled by means of a water bath.

3) S. P. CLARK, Jr., *Trans. Amer. Geophys. Union*, **38** (1957), 931. *Bull. Geol. Soc. Amer.*, **17** (1956), 1123.

4) H. A. LUBIMOVA, *Akad. Nauk SSSR, Inst. Fiziki Zemili Trudy*, **178** (1960), 72.

5) A. E. BENFIELD, *Proc. Roy. Soc. London A*, **173** (1939), 428.

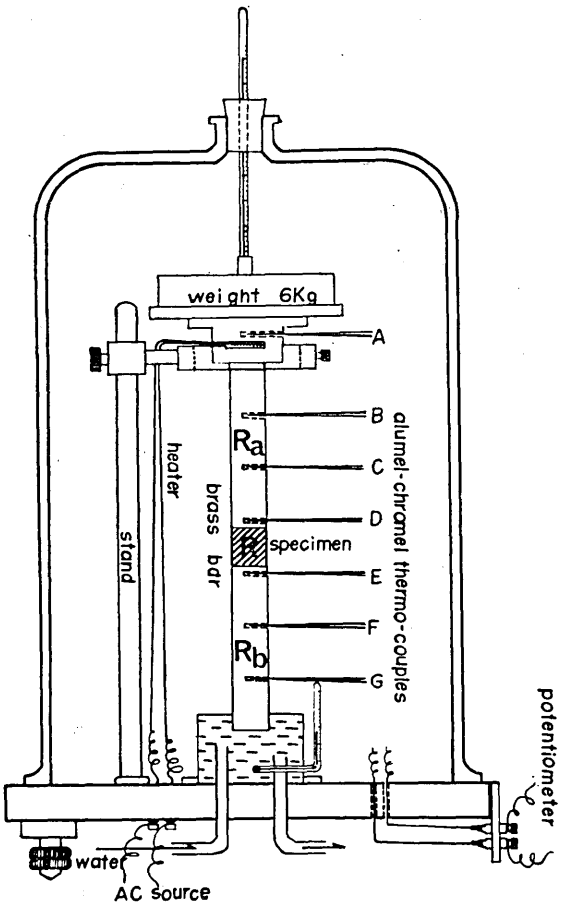

Fig. 1. Divided-bar device for measurement of thermal conductivity of rocks.

The temperatures at points A, B, C, D, E, F, and G are measured by thermocouples placed in small holes.

In the steady state, and if there are no radial heat losses, the amount of heat flowing down the ensemble R_a-R-R_b is constant at all places, and if we denote this by H,

$$H=K_bP_b=K_rP_r\ ,$$

where K_b and K_r are the conductivities of the metal and rock respectively, and P_b and P_r the corresponding temperature gradients.

Hence, K_r can be determined when K_b, P_r, P_b have been measured.

However, when this divided bar method is used for the measurement of the thermal conductivity of rocks, the time for a new specimen to reach the thermal stationary state is usually in excess of one hour. In order to shorten the time, Beck[6] made a modification. In the modified divided bar method, heat is supplied to the upper end of bar (R_a) by means of a thermostatically controlled heater and the lower end of bar (R_b) is cooled also by a thermostatically controlled heat sink. This, being a "constant temperature" system in contrast to the former "constant heat" system, reduced the time constant of the whole apparatus, when the specimen is changed, to some ten minutes. Such a modified apparatus has been used for the measurement of thermal conductivity of rocks in the work on the terrestrial heat-flow in Japan[7].

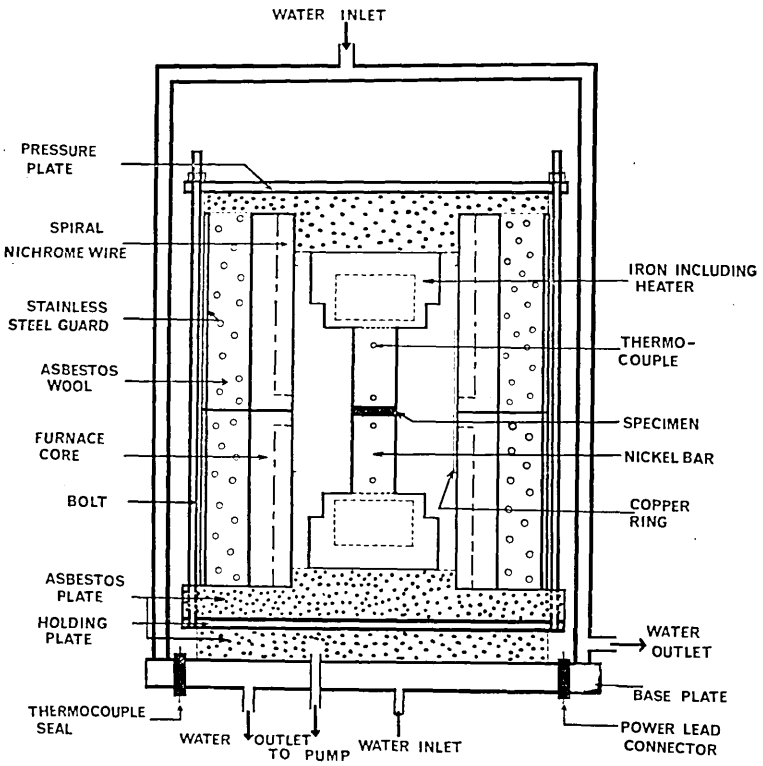

Fig. 2. Modified divided-bar device for measurement of thermal conductivity of rocks.

6) A. E. BECK, *J. Sci. Instr.*, **34** (1957), 186.
7) K. HÔRAI, *Bull. Earthq. Res. Inst.*, **42** (1964), 93.

For the present purpose of measuring the thermal variation of rocks, however, the apparatus described above cannot be used directly. Several years ago, the divided bar apparatus was improved for high temperature measurements of the thermal conductivity of dielectric substances by I. Yoshida at the Tokyo Institute of Technology[8]. Our present apparatus is a modified version of Yoshida's apparatus. A schematic representation of the arrangement of the present apparatus is shown in Fig. 2.

In our apparatus, nickel bars were used as the reference substance, because nickel stands the effect of oxidation at high temperature and its thermal conductivity at high temperatures is comparatively well known. The nickel bars were made 2 *cm* in diameter and 4 *cm* in length. Into each bar two radial holes 0.3 *cm* in diameter and 0.5 *cm* deep were drilled. The holes were spaced along the bar at 2.5 *cm* intervals and one of the holes was drilled 0.5 *cm* away from the end facing the sample disk. Each of the bars is connected by a screw with an iron piece containing an auxiliary electric heater. The iron piece is 6 *cm* in diameter, and 3.5 *cm* in thickness. This has a hollow, having a 4 *cm* diameter and 2 *cm* depth, in which the auxiliary electric heater with a nichrome wire (0.003 *cm* in diameter) is inserted. The auxiliary heaters thus placed at both ends of the system are to give the temperature gradient in the system. Around the bars, four main electric furnaces are set. These four electric furnaces are so placed that they form a concentric cylinder. Each electric furnace core has a 7.5 *cm* internal diameter and an 11 *cm* outer diameter. Around this core, there is a stainless steel guard, and asbestos wool fills the space between the heater core and the guard. The stainless steel guard serves as a reflector of radiative heat. Spiral nichrome wire, 0.1 *cm* diameter 400 *watts*, lies in the grooves of the inner face of each furnace, therefore, in total, the main heater has a power of 1600 *watts*. The bars and furnaces are placed on a piled asbestos plate about 1 *cm* thick. All of these are, then, set on a holding plate which sits on another asbestos plate, 2 *cm* thick. To avoid oxidization of the apparatus and the specimen, the whole system is evacuated to 10^{-2}–10^{-3} *mmHg* throughout the experiment. To secure a good thermal contact between the bar and specimen, silver paste is used, and in addition, an axial pressure applied by means of screws on the pressure plate. The thermocouples and power leads are hermetically jointed with the base

8) I. YOSHIDA, *J. Phys. Soc. Japan*, **69** (1961), 2121.

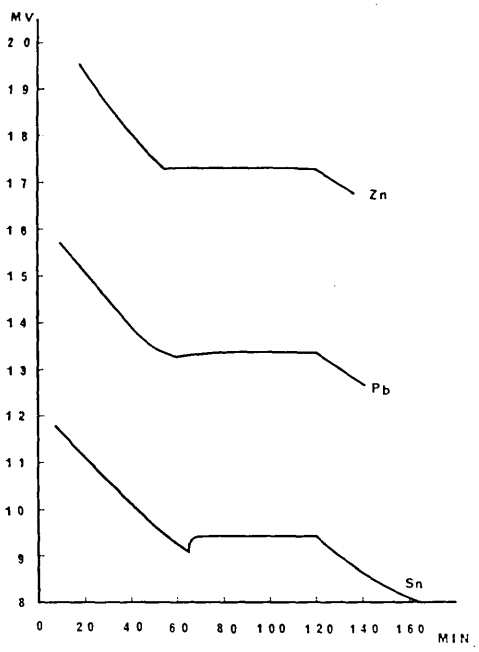

Fig. 3. Examples of solidification curves.

plate. The thermocouples used are chromel and alumel wire of 0.06 *cm* diameter. The calibration of thermocouples was made by the solidifying point of pure liquid metals; *Sn*, *Pb*, *Zn*, and *Sb*. Examples detecting the solidification temperature are shown in Fig. 3, which is the automatic record of the time variation of the thermo *e.m.f.* of the thermocouple measured in the liquid metal which is slowly cooling. It may be clearly seen that the *e.m.f.* was kept constant for about half an hour during the furnace-cooling of the crucible containing the liquid metal. A Yokokawa Co. precision potentiometer was used for *e.m.f.* readings of the thermocouples. Readings were taken to 1 μV while approximately 40 μV corresponds to 1°*C* for all the thermocouples throughout the temperature range studied (0°*C*—600°*C*).

The specimen disks were cut from the rocks with a diamond saw and drill and both surfaces were polished flat by hand. The surfaces were made as parallel as possible; the difference in thickness measured at various points was always made less than 1/25 of the thickness.

2-2. Operation of Experiment

In actual experiments the temperature reading in the bars was taken after the steady state had been reached. Then, the thermal conductivity of the specimen is determined in terms of the conductivity of the nickel bars. The effect of the thermal contact resistance between the bars and the specimen was eliminated by measurements with two or more disks of different thicknesses. In our apparatus, the time for a single specimen to reach a stationary state at high temperatures was three or more hours.

In order to make the thermal gradients in the upper and lower

bars equal, the electric currents in the main and auxiliary heaters were manually adjusted with variable auto-transformers. This operation required much skill and experience. After many trials, the best combinations of currents and voltages were determined for each desired temperature. For instance, to keep the specimen temperature at about 100°*C* the upper auxiliary heater voltage being at 30 *V*, after one hour, they are changed to 1 ampere, 10 *V*, then after another hour to 0.8 ampere, and 8 *V* respectively. Operating conditions for other temperatures were determined likewise and tabulated in Table 1.

Table 1. Operating condition of electric furnaces.

Heater	Start	1 hour	2 hour	Temperature
Upper furnace	2 *A*	1 *A*	0.8 *A*	about 100°*C*
Lower furnace	2 *A*	1 *A*	0.8 *A*	
Upper auxiliary	30 *V*	10 *V*	8 *V*	
Lower auxiliary	0 *V*	0 *V*	0 *V*	
Upper furnace	2.5 *A*	1.5 *A*	1.1 *A*	about 250°*C*
Lower furnace	2.5 *A*	1.5 *A*	1.1 *A*	
Upper auxiliary	30 *V*	20 *V*	20 *V*	
Lower auxiliary	0 *V*	0 *V*	0 *V*	
Upper furnace	3.5 *A*	2.5 *A*	1.8 *A*	about 450°*C*
Lower furnace	3.5 *A*	2.5 *A*	1.8 *A*	
Upper auxiliary	40 *V*	25 *V*	20 *V*	
Lower auxiliary	0 *V*	0 *V*	0 *V*	
Upper furnace	4.5 *A*	3.5 *A*	2.2 *A*	about 600°*C*
Lower furnace	4.5 *A*	3.5 *A*	2.2 *A*	
Upper auxiliary	50 *V*	30 *V*	25 *V*	
Lower auxiliary	0 *V*	0 *V*	0 *V*	

2-3. Theory

In the steady state, and if there are no radial heat losses, the amount of heat flowing along the bar, Q, is constant. Therefore, denoting various quantities as indicated in Fig. 4.

$$Q=K_1\frac{\theta_1-\theta_2}{2.5}=K_1\frac{\theta_2-\theta_3}{0.5}=K_2\frac{\theta_3-\theta_4}{t_1}=K_3\frac{\theta_4-\theta_5}{D}$$
$$=K_2\frac{\theta_5-\theta_6}{t_2}=K_1'\frac{\theta_6-\theta_7}{0.5}=K_1'\frac{\theta_7-\theta_8}{2.5}, \qquad (2\text{-}1)$$

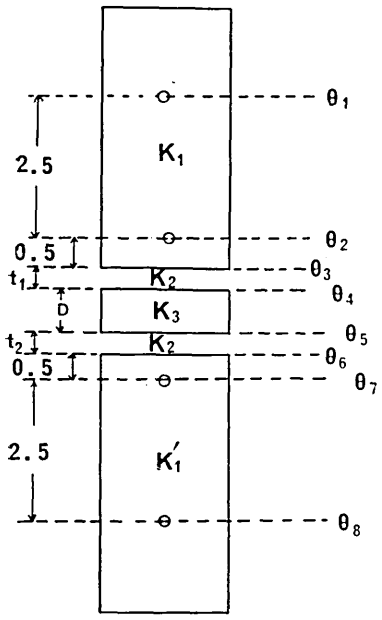

Fig. 4. "Constant temperature difference" divided-bar apparatus.

where, K_1, K_1', K_2, K_3 are the conductivities of the upper and lower parts of the nickel bars, interface gap, and the sample. θ, t_1, t_2, and D are temperatures, the thickness of the interface gaps, and the sample thickness. Also,

$$\theta_2-\theta_7=(\theta_2-\theta_3)+(\theta_3-\theta_4)+(\theta_4-\theta_5)+(\theta_5-\theta_6)+(\theta_6-\theta_7)\,, \tag{2-2}$$

thus, from equations (2-1) and (2-2)

$$\frac{1}{K_1}\left\{\frac{2.5(\theta_2-\theta_7)}{\theta_1-\theta_2}-0.5\right\}=\frac{t_1+t_2}{K_2}+\frac{D}{K_3}+\frac{0.5}{K_1'} \tag{2-3}$$

$$\frac{1}{K_1'}\left\{\frac{2.5(\theta_2-\theta_7)}{\theta_7-\theta_8}-0.5\right\}=\frac{t_1+t_2}{K_2}+\frac{D}{K_3}+\frac{0.5}{K_1} \tag{2-4}$$

therefore

$$\frac{D}{K_3}=\frac{1}{K_1}\left\{\frac{2.5(\theta_2-\theta_7)}{\theta_1-\theta_2}-0.5\right\}-\frac{t_1+t_2}{K_2}-\frac{0.5}{K_1'} \tag{2-5}$$

$$\frac{D}{K_3}=\frac{1}{K_1'}\left\{\frac{2.5(\theta_2-\theta_7)}{\theta_7-\theta_8}-0.5\right\}-\frac{t_1+t_2}{K_2}-\frac{0.5}{K_1}\,. \tag{2-6}$$

Thus K_3 is determined from the temperature gradients in both the upper bar and the lower bar independently. These two determinations are averaged to get the K_3 value for the temperature.

3. Calibration of Nickel

There is no compelling reason except the following to choose nickel as the reference substance. At first, the reference substance was brass. However, the variation of thermal conductivity of brass has been measured only at temperatures below 80°C and, moreover, at high temperatures brass is easily oxidized. For this reason, it was considered undesirable to use brass as the reference substance at high temperatures. Variation of thermal conductivity of nickel, on the other hand, has been measured by many researchers, and it is not easily oxidized. However, the values of thermal conductivity of nickel over high

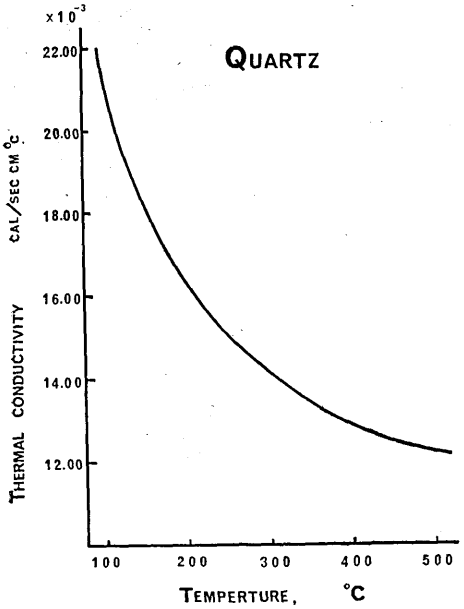

Fig. 5. Thermal conductivity of quartz (after A. Goldsmith *et al.*).

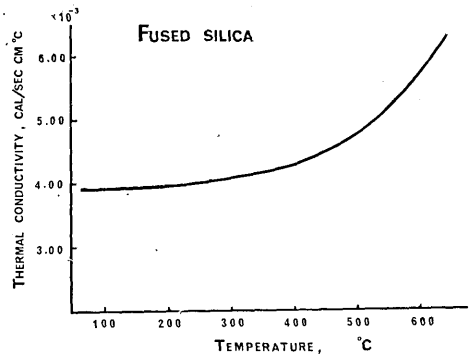

Fig. 6. Thermal conductivity of fused silica (after A. Goldsmith *et al.*).

Table 2. Thermal conductivity of nickel.

Temperature (°C)	Thermal conductivity (*cal/sec. cm. °C*)		Temperature (°C)	Thermal conductivity (*cal/sec. cm. °C*)	
	Fused silica	Nickel		Quartz	Nickel
114.4	0.00390*	0.133	104.6	0.02080*	0.131
	0.00390*			0.02075*	
122.6	0.00390′	0.132	106.5	0.02080′	0.130
	0.00390′			0.02075′	
190.2	0.00395*	0.125	253.1	0.01500*	0.119
	0.00394*			0.01490*	
206.8	0.00395′	0.123	256.9	0.01500′	0.118
	0.00394′			0.01490′	
255.8	0.00402*	0.119	454.0	0.01247*	0.112
	0.00401*			0.01246*	
275.6	0.00402′	0.116	458.3	0.01247′	0.113
	0.00401′			0.01246′	
454.3	0.00454*	0.113	509.2	0.01222*	0.116
	0.00453*			0.01222*	
469.3	0.00454′	0.114	514.4	0.01222′	0.117
	0.00453′			0.01222′	
575.1	0.00562*	0.121			
	0.00553*				
591.7	0.00562′	0.123			
	0.00553′				

(*) and (′) signs show a measured value at the upper and the lower bars respectively.

temperatures, listed in various tables, differ considerably. Therefore, in any case, the change of the thermal conductivity of the particular nickel to be used as the reference had to be determined.

It was later found by Moss that[9], there is an abrupt change in the thermal conductivity of nickel at the temperature of the Curie point. Such an anomalous behaviour is also reported in the Handbook of Thermophysical Properties of Solid Materials[10]. Naturally, it would

Table 3. Chemical analysis of nickel.

Investigator	Range, (°C)	Material composition	Test method	Remarks
L. Silverman,	53—910	Grade A; 98.19% Ni; 0.746% Co; 0.705% Mo; 0.26% Fe; 0.063% Cu; 0.036% P.	Comparative; rods.	Used Pb as primary standard, "Advance" as working standard.
M. Moss,	103—567	0.094% Si; 0.082% Cu; 0.056% Fe; 0.027% C; 0.025% Co; 0.008% S; 0.007% Al.	Comparative; rods.	
P. O. Davey, and G. C. Danielson,	153—644	Grad A; 99.542% Ni; 0.250% Mn; 0.068% Fe; 0.034% Co; 0.034% Mg; 0.030% Si; 0.020% Ti; 0.014% Cu; 0.006% Al; 0.001% B; 0.0005% Ca; 0.0005% Cr.	Comparative; rods; Peened thermocouples.	Vacuum of 2×10^{-5} *mmHg*.
C. L. Hogan, and R. B. Sawyer,	3—910	99.48% pure; 0.22% Mn; 0.14% Fe; 0.06% C; 0.05% Cu; 0.02% Si; 0.005% S.	Tem. distribution in rod heated at one end; meas. heat losses from surface.	
K. Kawada	100—630	99.244 *wt*% Ni; 0.56% Mn; 0.079% Fe; 0.040% Cu; 0.022% Ti; 0.022% Si; 0.02% C; 0.008% Co; 0.003% S; 0.002% Mg.	Comparative; rods.	Vacuum of 10^{-2}—10^{-3} *mmHg*

9) M. MOSS, *Rev. Sci. Instr.*, **26** (1955), 276.

10) A. GOLDSMITH, *et al.*, *Handbook of Thermophysical Properties of Solid Materials*, Vol 1, (Macmillan Company, New York, 1961).

be more desirable to choose a metal that has no such anomalous nature, but, in the absence of any better materials at hand, we made use of nickel as the reference substance. The thermal conductivity of nickel at various temperatures was calibrated by using disks of crystalline quartz (X cut) and fused silica, instead of rock specimens. These substances are definite ones and the variation of their thermal conductivities determined by various authorities are quite reliable and concordant. In practice, we adopted the values listed in the tables of the Handbook of Thermophysical Properties of Solid Materials (see Figs. 5 and 6.). The thermal conductivity of nickel is determined from equations (2-3) and (2-4),

$$\frac{1}{K_1}\left[\left\{\frac{2.5(\theta_2-\theta_7)}{\theta_1-\theta_2}-0.5\right\}-\left\{\frac{2.5(\theta_2'-\theta_7')}{\theta_1'-\theta_2'}-0.5\right\}\right]=\frac{1}{K_3}(D-D') \qquad (3\text{-}1)$$

and

$$\frac{1}{K_1'}\left[\left\{\frac{2.5(\theta_2-\theta_7)}{\theta_7-\theta_8}-0.5\right\}-\left\{\frac{2.5(\theta_2'-\theta_7')}{\theta_7'-\theta_8'}-0.5\right\}\right]=\frac{1}{K_3}(D-D') \qquad (3\text{-}2)$$

where K_3 is the thermal conductivity of crystalline quartz and fused silica. Table 2 shows the experimental result. The nickel used for the

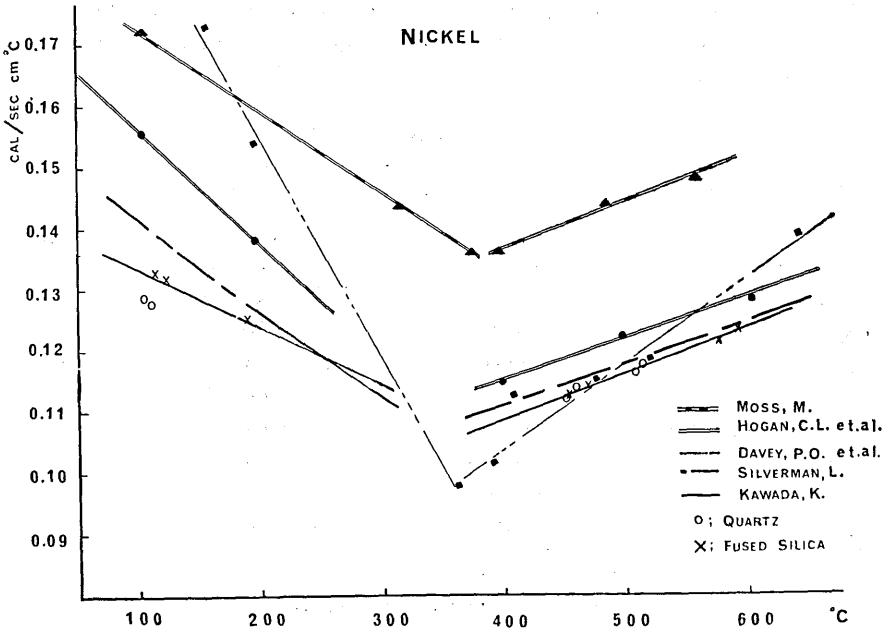

Fig. 7. Thermal conductivity of nickel.

present study is 99.244 percent. The results of the chemical analysis and thermal conductivity of the nickel are shown in Table 3 and Fig. 7. The difference of thermal conductivity of nickel obtained by many workers may be due to different impurities in the metals.

4. Description of Materials

According to seismologists, the longitudinal wave velocity jumps abruptly to 8.2 *km/sec* from 6.5 *km/sec* at the Moho discontinuity. It is not known for certain what kind of rocks form both sides of the Moho discontinuity. However, the laboratory experiment on the propagation velocity of longitudinal and transverse waves indicates that peridotite and eclogite are the only common rocks which possess the sonic velocity, $V=8.2$ *km/sec.* while rocks with the sonic velocity, $V=6.5$ *km/sec,* are gabbro, basalt, serpentine and so on. From the above, it may be considered that dunite, peridotite and eclogite used in the present study are the substances constituting characterizing the mantle, and basalt and gabbro the main constituent materials of the lower parts of the continental crust and the oceanic crust. The remaining major crustal substances; serpentine, diorite, quartz-diorite and slate are used in order to determine the temperature distribution within the crust beneath Japan. Table 4 gives the names of these specimens, their places of origin, collectors, and their density.

Table 4. Rock specimens

Rock type	Place of origin	Collector	Density (g/cm^3)
Dunite	Kyushu	S. Uyeda	3.21
Peridotite (1)	Mie	T. Nakamura	3.05
Peridotite (2)	Mie	T. Nakamura	2.95
Eclogite	Aichi	H. Kuno	3.50
Basalt	Kyushu	S. Uyeda	2.58
Hornblende-gabbro	Kyoto	H. Kuno	3.06
Serpentinized-peridotite	Iwate	H. Kuno	2.74
Quartz-diorite	Hokkaido	H. Kuno	2.64
Diorite	Iwate	H. Kuno	2.92
Slate	Fukushima	H. Kuno	2.70

5. Experimental Results

The calculation of the thermal conductivity of rocks from the

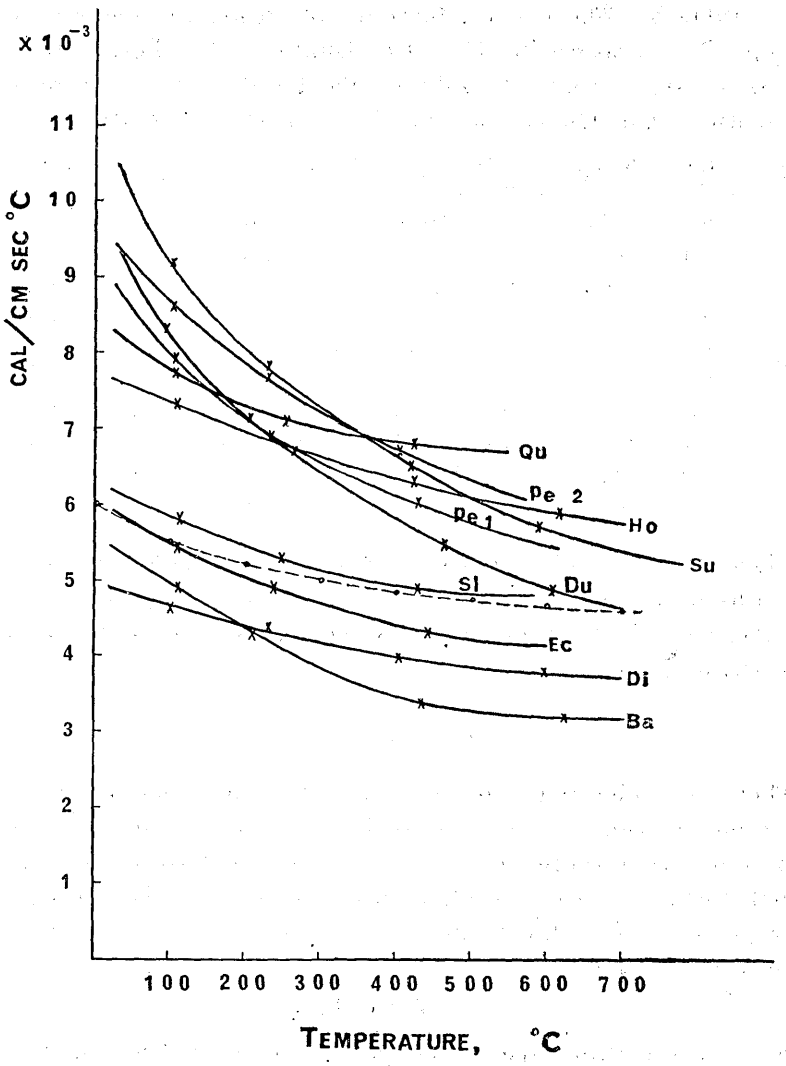

Fig. 8. Thermal conductivity of rocks.

experimental readings was carried out by equations (2-5) and (2-6). The results are shown in Table 5 and Fig. 8, in which the values of the thermal conductivity are plotted against the temperature. The amount of possible error of each point is estimated to be about $\pm 10\%$.

As can be observed in the figure, all the specimens showed a smooth decrease of thermal conductivity with the increase in temperature. This tendency is in good agreement with the results of Birch

Table 5. Thermal conductivity of rocks. (*cal/cm. sec.* °*C*)
Temp.: Temperature in °*C*. Du: Dunite. Pe: Peridotite. Ec: Eclogite. Ho: Hornblende-gabbro. Ba: Basalt. Se: Serpentinized-peridotite. Qu: Quartz-diorite. Di: Diorite. Sl: Slate.

Temp. (°C)	Du ($\times10^{-3}$)	Temp. (°C)	Pe (1) ($\times10^{-3}$)	Temp. (°C)	Pe (2) ($\times10^{-3}$)	Temp. (°C)	Ec ($\times10^{-3}$)	Temp. (°C)	Ho ($\times10^{-3}$)
93.1	8.3	107.8	7.9	101.0	8.6	110.9	5.4	107.7	7.3
204.1	7.1	264.2	6.7	232.4	7.7	236.6	4.9	232.0	6.9
462.5	5.4	429.7	6.0	402.2	6.7	443.2	4.3	424.0	6.3
608.6	4.9							614.8	5.9
Temp. (°C)	Ba ($\times10^{-3}$)	Temp. (°C)	Se ($\times10^{-3}$)	Temp. (°C)	Qu ($\times10^{-3}$)	Temp. (°C)	Di ($\times10^{-3}$)	Temp. (°C)	Sl ($\times10^{-3}$)
110.6	4.9	100.7	9.2	107.3	7.7	103.6	4.6	111.3	5.8
208.0	4.3	230.3	7.8	253.7	7.1	232.4	4.4	247.4	5.3
433.2	3.4	419.3	6.5	424.5	6.8	402.2	4.0	426.7	4.9
622.3	3.2	590.2	5.7			598.8	3.8		

and Clark. No sign of increase in thermal conductivity due to radiative effect was observed in the present study, but it is quite reasonable as the radiative effect is supposed to be appreciable only in a higher temperature range.

6. Discussion

Thermal conductivity in solids is determined mainly by electronic and atomic motions. For the rocks, it is clear, from low electrical conductivity, that there are only a few free electrons; the transfer of thermal energy is attributable almost entirely to the motions of the lattice particles, *i. e.* the phonon. In such a case, the thermal conductivity is given by

$$K=ACV\lambda$$

where, C is the heat capacity per unit volume, V the sound velocity, λ the mean-free-path of phonon and A the constant factor[11].

The mean-free-path of phonon is determined principally by two processes, *i. e.* the scattering geometrically and by other phonon. If the forces between atoms were purely harmonic collisions among phonons would not occur, the mean-free-path being restricted only by scattering of phonon with the crystal boundaries, and lattice imperfections. But however, such a scattering effect is known, for some

11) C. KITTEL, *Introduction to Solid State Physics*, (John Wiley and Sons, Inc., New York, 1956), pp. 139.

substances, to become important only at very low temperatures. With an harmonic lattice interactions there is a coupling between different phonons and the mean-free-path of phonon is restricted. It is this an harmonic nature of the lattice vibration that is believed to produce finite conductivity of heat in solids. This problem was discussed in great detail by Peierls[12]; according to his theory, at high temperatures the mean-free-path of phonons is inversely proportional to the absolute temperature, $1/T$. On the other hand, according to the theories of Pomeranchuk and Lubimova[13] it varies as $T^{-3/2}$ and $T^{-5/4}$. These theoretical $K-T$ relations have been found to be in agreement, at least qualitatively, with the experimental results reported here: In either case, it is clear that the thermal conductivity decreases with the temperature increase. Therefore, as regards the present experiments, it may be unquestionable that phonons play a role in silicate rocks at temperatures below 600°C.

Geometrical effects might also be important in limiting the mean-free-path of phonons. Here, we must also consider scattering by crystal boundaries, lattice imperfections, and amorphous structures. Unfortunately, in the present stage, discussion of this kind is difficult, mainly due to the scarcity of data at low temperatures. It is intended to make measurements on many more specimens and in wider temperature ranges in the near future. Present results cannot be used for the problems of heat transfer in the mantle as the temperature in the mantle is supposed to be more elevated than that covered in the present study. Instead, the present results may be used for the estimation of temperature distribution within the crust. Using the heat-flow values in Japan as measured by Uyeda and Hôrai[14] and Bullard's summary of the standard values of the radioactive heat production of common rocks as referred to by Uyeda and Hôrai, and the model of the crust under Japan adopted by the same authors[14], the temperature distribution from surface to Moho discontinuity can be calculated by the following formula[15]

$$\begin{aligned} T_{i+1} &= T_i + \frac{1}{K_i}\left(Q_i - \frac{1}{2}H\cdot\Delta D\right)\cdot\Delta D\,, \\ Q_{i+1} &= Q_i - H\cdot\Delta D\,, \end{aligned} \tag{6-1}$$

12) R. PEIERLS, *Quantum Theory of Solids*, (Clarendon Press, Oxford, 1955), Ch. 2.
13) H. A. LUBIMOBA, *Geophys. J.*, **1** (1958), 115.
14) S. UYEDA, and K. HÔRAI, *J. Geophys. Res.*, **69** (1964), 2121.
15) K. HÔRAI, *ibid.*, 634.

Table 6. Regional thermal characteristics of Japan. (after Uyeda and Hôrai)

Region	Crustal thickness, km	Heat-flow in 10^{-6} cal per cm^2 sec			Temperature at 1 km Depth, °C	Heat flow Divided by Crustal Thickness, $\times 10^{-12}$ cal/cm^3 sec	Estimated Temperature at M Discontinuity, °C			
		Observed Q_{obs}	Calculated Q_{cal}	Q_{diff}			T_1	T_2	T_1*	T_2*
A, Pacific side of northeastern Japan	23	0.65	0.93	−0.28	20	0.28	233	147	267	109
B, Japan Sea side of northeastern Japan	27	2.20	1.09	+1.11	40	0.81	1146	816	1673	534
C, Central Honshu	39	1.80	1.57	+0.23	35	0.46	1297	716	1823	531
D, Central and Pacific parts of southwestern Japan	29	1.20	1.17	+0.03	30	0.41	605	346	781	266

(T_1 and T_2: Temperatures which are obtained by assuming respectively the minimum and maximum rates of heat production). (T_1*, T_2*: calculated by Kawada).

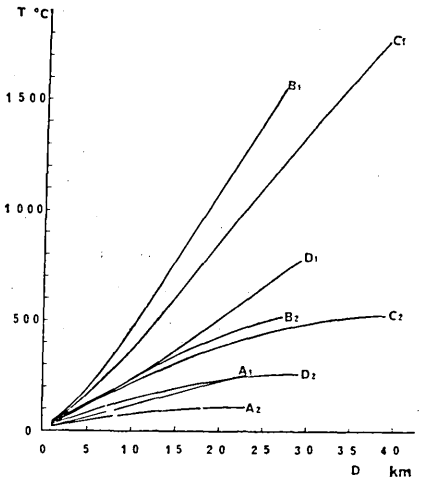

Fig. 9. Temperature-depth curves in the crust.

where, T_i is the temperature at the upper face of the ith layer, Q_i the heat flowing through the upper face of the ith layer, and K_i the thermal conductivity within the ith layer. K_i is assumed to be constant in the ith layer and the experimental results obtained here are used. D is the thickness of each layer ($=2\,km$). H the rate of heat production.

We now use the measured thermal variation of thermal conductivity while Uyeda and Hôrai used the average $K-T$ relation taken from the data by Birch and Clark. The $K-T$ relation assumed by Uyeda and Hôrai is plotted by the dotted line Fig. 8. It may be noted that, by the use of present experimental results, the possible

ranges of the temperature in the crust became wider than those estimated by Uyeda and Hôrai. The results of the calculations are shown in Table 6 and Fig. 9.

Acknowledgment

The author would like to express his thanks to Prof. T. Rikitake and Dr. S. Uyeda by whose constant advice, discussion and encouragement the present work has been made.

---

35. 地球熱学 第15報
岩石の熱伝導率の温度変化　その1

地震研究所　川　田　　薫

ダンかんらん岩，かんらん岩，榴輝岩，角閃石一かんらん岩，石英片岩，片岩およびねん板岩の熱伝導率を，改良した divided-bar 装置で 100°C から 600°C の温度範囲で測定した．

標準物質にはニッケルを用い，石英と溶融石英で検定した．すべての岩石の熱伝導率は温度の増加と共に一様に減少し，この現象はフォノン熱伝導で定性的に説明可能である．

岩石の熱伝導率の測定結果は地殻中の温度分布を決定するのに使われた．